Delone clusters, covering and linkage in the quasiperiodic triangle tiling

2000 J. Phys. A: Math. Gen. 33 7885

(http://iopscience.iop.org/0305-4470/33/44/304)

J. Phys. A: Math. Gen. **33** (2000) 7885–7901. Printed in the UK PII: S0305-4470(00)12489-8

Delone clusters, covering and linkage in the quasiperiodic triangle tiling

Peter Kramer
Institut für Theoretische Physik der Universität, D 72076 Tübingen, Germany

Received 6 March 2000

Abstract. The triangle and the Penrose tiling are dual quasiperiodic projections from the root lattice A_4. The dual-window theory is developed and applied to pentagonal Delone clusters in the triangle tiling. The filling, covering, fundamental domain and linkage properties of Delone clusters are analysed.

1. Introduction

In 1987 Conway, as quoted by Grünbaum and Shepard [2, p 562], gave a theorem on the Penrose tiling: every Penrose triangle tiling is covered by congruent decagonal patches, called cartwheels. This theorem led Gummelt [4] to the interpretation of Penrose tilings as coverings of congruent decagons. Jeong and Steinhardt [12] developed the decagon covering for the description of atomic positions in decagonal quasicrystals and related it to the notion of a unit cell.

Why are coverings of interest for the atomic structure of quasicrystals? Suppose that a tiling in position space can be covered by a few clusters with linkage rules. In the spirit of Conway's theorem, it would follow that the tiles in the tiling are correlated in patches formed by these clusters. In other words, there is much more local rigidity in the tiling than what one would expect from the matching of next-neighbour tiles. Consequently, the atomic positions in the tiling model must be correlated over the full range of these clusters. From the coverings one would therefore hope to gain new and simpler views on the structure and physics of quasicrystals.

With this motivation, it seems reasonable to explore rigorous results on clusters and coverings from tiling theory. To this end we start from independent notions for clusters, coverings, linkages and fundamental domains and then study their relations. The experience with dual projected quasiperiodic tilings (see [6] for general properties) suggests the technique of windows. This technique is applied to covering problems in [8]. Voronoi and Delone clusters are taken as parallel projections of Voronoi and Delone cells. The Penrose and triangle tilings are dual projections from the root lattice $\Lambda = A_4$. The decagons of Gummelt [4] in the Penrose tiling are Voronoi clusters [8] (see also [9]). The triangle tiling has been applied to the structure and physics of decagonal quasicrystals, for example, to the local electronic structure in AlCuCo [7]. Pentagonal Delone clusters in the triangle tiling are introduced in [8, section 5 and appendices A, B]. They are studied here by new methods, in much more detail, and with new results. The cell geometry and holes of the lattice A_4 and the triangle tiling $(\mathcal{T}^*, A_4)$ are briefly described in section 2. In section 3 we give a full algebraic analysis of the windows

0305-4470/00/447885+17$30.00

for Delone clusters. The new constructive definition in proposition 1 for the filling by tiles of a Delone cluster and its window is independent of the cluster position in the tiling. When related to the tiling it yields all occurrences of the filled Delone cluster viewed from any of its vertices. A corresponding total window reflects these views, the window given in [8] describes only a particular one. General criteria for the covering by Delone clusters of vertices and tiles in the tiling are given in section 4. From the total windows it is shown that any vertex and any tile in the triangle tiling is covered by at least one Delone cluster. The covering fraction is computed explicitly. In section 5 we summarize the relation between Delone clusters and a fundamental domain for the tiling found in [8]. Section 6 deals with the linkage of Delone clusters. All possible linkages of Delone clusters by a vertex and their relative frequencies are constructed from their windows and characterized algebraically.

2. The triangle tiling ($\mathcal{T}^*$, A_4)

We refer to [3] for the geometry of lattices and to [1] for a detailed description of the root lattice A_4, its geometry and its projection. In terms of five orthonormal vectors $\langle e_1, \ldots, e_5\rangle \subset E^5$ we form the five vectors

$$a_j := e_j - \tfrac{1}{5}\sum_1^5 e_l \qquad j = 1, \ldots, 5 \qquad \sum_1^5 a_i = 0 \tag{1}$$

with one linear relation to express all relevant positions in the root lattice $A_4 \subset E^4$. The lattice points $q \in A_4$ are then given by those integral linear combinations of the vectors (1) whose sum of coefficients are equal to 0 mod 5. Reasons for the use of the vectors equation (1) rather than a lattice basis are given in and after definition 1. In the root lattice we construct the Voronoi cells $V(q)$ centred at all lattice points q and the set of dual Delone cells D^h centred at all hole positions h (cf [3, p 33]), which form the vertices of $V(q)$. The Voronoi cell $V(q)$ is bounded by hyperplanes at an equal distance between pairs of neighbouring lattice points. Any face or boundary X of dimension l, $0 \leqslant l \leqslant 4$, from $V(q)$, termed an l-boundary in the terminology of Sommerville [11, p 96], is uniquely determined by an intersection of hyperplanes between a minimal set $s(X) := \langle q'\rangle(X)$ of lattice points. Its dual $(4-l)$-boundary X^* is defined [6] as the convex hull $X^* := \langle \mathrm{conv}(q'), q' \in s(X)\rangle$. It is the face or boundary of a dual Delone cell [3, p 35]. The holohedry or full point group of A_4 is $S_5 \times Z_2$ generated by the permutations of S_5 and by the inversion $i = (1\bar{1})(2\bar{2})(3\bar{3})(4\bar{4})(5\bar{5})$. We express all actions of the point group as signed permutations of the vectors $\langle a_1, \ldots, a_5\rangle$.

To characterize the (shallow and deep) holes in the lattice A_4 (cf [3, pp 108–10]) we introduce, seen from the points q of the lattice, the hole positions

$$h = \sum_1^5 n_j a_j \tag{2}$$

and the modulo function

$$r(h) = \sum_1^5 n_j \bmod 5. \tag{3}$$

Definition 1. *The shallow holes h of the root lattice A_4 are denoted by the letter $h = a$. They are the point classes $(h, r(h)) = (a, 1), (a, 4)$. The deep holes are denoted by the letter $h = b$. They are the point classes $(h, r(h)) = (b, 3), (b, 2)$. The inversion i is a rotation by π both in $E_\parallel$, $E_\perp$. Under this operation, the pairs of shallow and deep hole classes interchange their role. The class q with $r(q) = 0$ describes the points of the lattice A_4.*

Any hole position h is a vertex or 0-boundary of a Voronoi cell and so can be written as the intersection of bounding hyperplanes between a minimal set of lattice points $s(h) := \langle q' \rangle$. The Delone cell dual to h is then $D^h = \langle \mathrm{conv}(q'), q' \in s(h) \rangle (h)$. Both the simple action of the point group and the unified description of hole and lattice points are our reasons for using the vectors $\langle a_1, \ldots, a_5 \rangle$ in equation (1) and not a lattice basis. The notation a_j for vectors with an index should be strictly distinguished from the notation for shallow and deep holes $h = a, b$. It can be shown that the point subgroup S_5 when acting with respect to any hole point belongs to the space group and hence to the symmetry group of A_4. We shall use this property in section 3.

The point subgroup compatible with the quasicrystal projection to the 2D parallel and perpendicular planes $E_\parallel$, $E_\perp$, $E_\parallel + E_\perp = E^4$ is the Coxeter group $I_2(5) < S_5$ in the notation of Humphreys [5, p 32], generated by the reflections $R_1 = (25)(34)$, $R_2 = (12)(35)$, enlarged by the inversion i. In the projection scheme for quasicrystals with fivefold point symmetry, the irrational plane $E_\parallel$ serves as position space and the irrational plane $E_\perp$ as the window space. The vectors a_j projected to these two planes form the two 5-stars shown in figure 1.

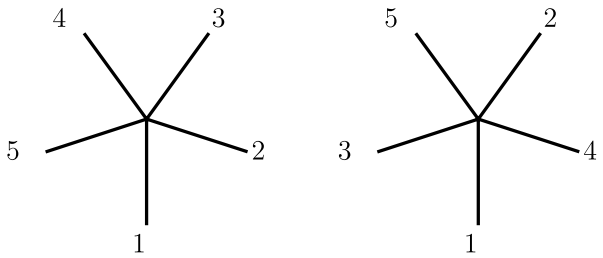

Figure 1. The vectors $\langle a_1, \ldots, a_5 \rangle$ form two 5-stars in $E_\parallel$ (left) and $E_\perp$ (right). They are used to describe the hole and lattice point positions of A_4 and their projections to these two spaces.

Definition 2. *The tiling* $(\mathcal{T}^*, A_4)$ *has the vertex set*

$$\{q_\parallel |\ q_\perp \in V_\perp\}. \tag{4}$$

The window $V_\perp$ *for the vertex set is the perpendicular projection of a fixed Voronoi cell. The tiles are dual 2-boundaries* $X^*_{1\parallel}$, $X^*_{2\parallel}$ *of Delone cells projected to* $E_\parallel$. *The windows for the tiles are 2-boundaries* $X_{1\perp}$, $X_{2\perp}$ *of the Voronoi cells projected to* $E_\perp$. *The tiles are two golden triangles, the windows are two Penrose rhombus tiles.*

3. Delone clusters in the triangle tiling

A Delone cell D^h in the lattice A_4 is a 4D polytope with its centre at a hole position h and equipped with a hierarchy of dual boundaries. A Delone cluster is defined in [8] as a parallel projection $D^h_\parallel$ of a Delone cell from the lattice A_4. It will be a polygon in $E_\parallel$. All dual boundaries of D^h if projected to $E_\parallel$ would overlap in a superposition with full symmetry under $I_2(5)$. Even the projection of all dual 2-boundaries would form such a superposition and would not be part of the tiling.

Definition 3. *A filling of (the polygon)* $D^h_\parallel$ *is a union of projected dual 2-boundaries* X^*_j *which covers* $D^h_\parallel$ *exactly and forms a patch of the tiling without gaps and overlaps.*

Dual tiling theory, as outlined in detail in [10], provides the construction given in proposition 1 for such a filling. It will be shown that this filling is unique, breaks the local symmetry inside the Delone cluster, and appears in the tiling with equal frequency in all orientations under $I_2(5)$.

Proposition 1 (Windows and fillings of Delone clusters). *Denote in $E_\perp$ by $X_{1\perp}(h)$, $X_{2\perp}(h)$ tiles in a standard orientation with a hole vertex of class h attached to a fixed hole position $h_\perp$. Determine by the application of point group elements g_l, $g_k \in I_2(5)$ with respect to the point $h_\perp$, compare section 2, a maximal intersection of tiles $g_l X_{1\perp}(h)$, $g_k X_{2\perp}(h)$ which share at least one interior point $x_\perp \neq h_\perp$. Construct in $E_\parallel$ by dualization and application of the same point group elements g_l, g_k the union of the dual tiles $g_l X^*_{1\parallel}$, $g_k X^*_{2\parallel}$. This intersection and this union are the window $w(h)$ and the filling $D^h_\parallel$ for a Delone cluster of fixed orientation,*

$$\begin{aligned} w(h) &= \cap_{l,k}(g_l X_{1\perp}(h))(g_k X_{2\perp}(h)) \\ D^h_\parallel &= \cup_{l,k}(g_l X^*_{1\parallel}(h))(g_k X^*_{2\parallel}(h)). \end{aligned} \tag{5}$$

We shall work out these expressions in the following subsections.

3.1. Standard positions of dual 2-boundaries

In $E_\perp$, $X_{1\perp}$, $X^*_{1\perp}$ are a thick rhombus and an obtuse triangle, $X_{2\perp}$, $X^*_{2\perp}$ are a thin rhombus and an acute triangle. We refer the standard positions to the centre $q = 0$ of a Voronoi cell. Each one of the boundaries X_1, X_2 with fixed orientation appears in three copies in a Voronoi window (cf figure 2). In the tiling $(\mathcal{T}^*, A_4) \subset E_\parallel$, these three copies are the windows for the triangle tiles X^*_1, X^*_2 seen from their three vertices, respectively. We drop the indices for parallel and perpendicular projections. This is allowed by the unique lifting property both from $E_\parallel$, $E_\perp$ to E^4. We express the boundaries in coordinates with respect to the centre q of a Voronoi cell and indicate this by writing $X_i(q)$, $X^*_i(q)$ (cf figure 2):

$$\begin{aligned} &X_1(q) := P(+0--0) := (a_1 - a_3 - a_4)/2 + (\lambda_2 a_2 + \lambda_5 a_5)/2 \\ &X^*_1(q) := \langle 0, a_1 - a_4, a_1 - a_3\rangle \\ &a_4 - a_1 + X_1(q) = a_4 - a_1 + P(+0--0) = P(-0-+0) \\ &a_4 - a_1 + X^*_1(q) = \langle a_4 - a_1, 0, a_4 - a_3\rangle \\ &a_3 - a_1 + X_1(q) = a_3 - a_1 + P(+0--0) = P(-0+-0) \\ &a_3 - a_1 + X^*_1(q) = \langle a_3 - a_1, a_3 - a_4, 0\rangle \\ &X_2(q) := P(+-00-) := (a_1 - a_2 - a_5)/2 + (\lambda_3 a_3 + \lambda_4 a_4)/2 \\ &X^*_2(q) := \langle 0, a_1 - a_2, a_1 - a_5\rangle \\ &a_2 - a_1 + X_2(q) = a_2 - a_1 + P(+-00-) = P(-+00-) \\ &a_2 - a_1 + X^*_2(q) = \langle a_2 - a_1, 0, a_2 - a_5\rangle \\ &a_5 - a_1 + X_2(q) = a_5 - a_1 + P(+-00-) = P(--00+) \\ &a_5 - a_1 + X^*_2(q) = \langle a_5 - a_1, a_5 - a_2, 0\rangle \\ &|\lambda_j| \leqslant 1. \end{aligned} \tag{6}$$

The notation is taken from [1], the triangles X^*_j are denoted by their vertex set. All other 2-boundaries are obtained from equation (6) by the action of the Coxeter group $I_2(5)$ and of i.

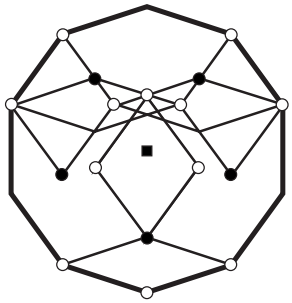

Figure 2. Positions for rhombus boundaries of fixed orientation in the decagonal Voronoi window $V_\perp$ with centre $q_\perp$, full square. The two standard positions $X_{1\perp}$, $X_{2\perp}$ have reflection symmetry under (25)(34). The hole vertex $(h, r(h)) = (a, 1)$ is marked on each rhombus by a full circle. The hole vertices $h = b$ are marked by open circles, the full class identification is given in figure 9.

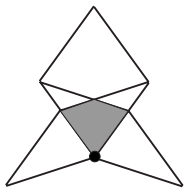

Figure 3. The window $w(a, 1)$ equation (8) for the Delone cluster $D_\parallel^{(a,1)}$ is the shaded intersection cone of three rotated rhombus tiles at a hole position $(h, r(h)) = (a, 1)$, full circle. The filling is given in figure 4.

3.2. Delone clusters $D_\parallel^a$ and their windows

Each tile X_1, X_2 has a single vertex of hole type $h = a$. For the Delone cluster it is convenient to rewrite the boundaries in coordinates with respect to this unique hole position. The vector for X_1, X_2 in standard position from $q = 0$ to this hole position is always $t = a_1$. Referred to the hole $(a, 1)$ we find for $X_i(a, 1)$, $X_i^*(a, 1)$

$$\begin{aligned} X_1(a,1) &= -a_1 + P(+0--0) \\ X_1^*(a,1) &= -a_1 + \langle 0, a_1 - a_4, a_1 - a_3\rangle \\ X_2(a,1) &= -a_1 + P(+-00-) \\ X_2^*(a,1) &= -a_1 + \langle 0, a_1 - a_2, a_1 - a_5\rangle. \end{aligned} \tag{7}$$

3.2.1. The window for fixed orientation of hole class $(a, 1)$. Upon choosing a particular orientation we arrive at expressions for the intersections and unions of tiles entering equation (5) as in table 1.

The combination of these tiles yields expressions for the window $w(a, 1) = w(D_\parallel^{(a,1)})$ and the filling $D_\parallel^{(a,1)}$ according to equation (5) in the form

$$\begin{aligned} w(a,1) &= (-a_1 + P(+0--0)) \cap (-a_2 + P(-+-00)) \cap (-a_5 + P(-00-+)) \\ D_\parallel^{(a,1)} &= (-a_1 + \langle 0, a_1 - a_4, a_1 - a_3\rangle) \cup (-a_2 + \langle 0, a_2 - a_3, a_2 - a_1\rangle) \\ &\quad \cup(-a_5 + \langle 0, a_5 - a_1, a_5 - a_4\rangle). \end{aligned} \tag{8}$$

It is understood that all expressions for windows refer to $E_\perp$ and all expressions for fillings refer to $E_\parallel$. The window $w(a, 1)$ is a cone at the hole $(a, 1)$ with an opening angle $2\pi/5$, taken from a decagon scaled by τ^{-2} with respect to $V_\perp$. It is shown in figure 3.

We now wish to characterize the filling $D_\parallel^{(a,1)}$ within the tiling $(\mathcal{T}^*, A_4)$. In terms of windows we must relate the window $w(a, 1)$ shown in figure 3 to the window $V_\perp$ for the tiling. In the present case it is possible to represent the window $w(a, 1)$ in particular as an intersection of rhombus tiles which belong to a single Voronoi window $V_\perp$. This is shown in figure 4(*a*), along with the filling $D_\parallel^{(a,1)}$ in (*b*).

Table 1.

Tiles $X_1(a,1)$, $X_1^*(a,1)$		
t	a_1	
g	e	
$gX_1(a,1)$	$-a_1 + P(+0--0)$	
$gX_1^*(a,1)$	$-a_1 + \langle 0, a_1 - a_4, a_1 - a_3\rangle$	
Tiles $X_2(a,1)$, $X_2^*(a,1)$		
t	a_1	a_1
g	(12345)	(15432)
$gX_2(a,1)$	$-a_2 + P(-+-00)$	$-a_5 + P(-00-+)$
$gX_2^*(a,1)$	$-a_2 + \langle 0, a_2 - a_3, a_2 - a_1\rangle$	$-a_5 + \langle 0, a_5 - a_1, a_5 - a_4\rangle$

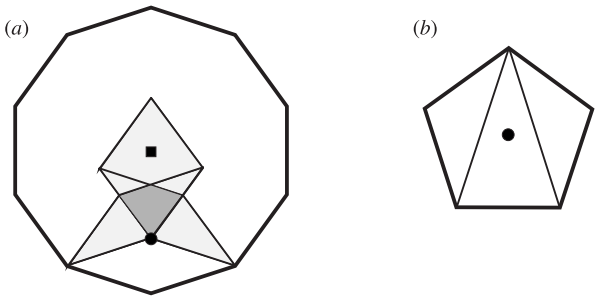

Figure 4. (*a*) Window cone $w(a,1)$: shaded, as an intersection of rotated rhombus tiles X_1, X_2 at a hole position $(h, r(h)) = (a,1)$; full circle, in the decagon $V_\perp$ centred at a lattice point $q_\perp$, full square. (*b*) Filled pentagonal Delone cluster $D_\parallel^{(a,1)}$ as union of the dual rotated triangles $X_{1\parallel}^*$, $X_{2\parallel}^*$.

3.2.2. All windows of hole class $(a,1)$ *for fixed orientation.* The contributing 2-boundaries X_l which intersect in the window $w(a)$ equation (7) refer to a variety of different Voronoi cells $V(q)$. To obtain the set of all lattice points q which participate in the union of tiles recall that the dual boundaries X_l^* are convex hulls for subsets of lattice points from this set. It follows that we find all the centres q of these Voronoi cells by collecting from table 1 all the different vertices of the dual tiles gX_1^*, gX_2^*. By inspection one finds, seen from the hole position $(a,1)$, the Voronoi centres

$$q - a = -a_1, -a_2, -a_3, -a_4, -a_5. \tag{9}$$

The inverses of these vectors are, by comparison with equations (2) and (3), five particular hole positions of type $(h, r(h)) = (a,1)$ belonging to $V(q)$.

Now we look for the general occurrence of the filling $D_\parallel^{(a,1)}$ with fixed orientation in the tiling. When checking the tiling vertex by vertex, one can identify a filling whenever one arrives at one of its vertices. Similarly, as we found for a single triangle tile three different rhombus windows within $V_\perp$ (see figure 2), corresponding to its three vertices, we expect to find for the filling $D_\parallel^{(a,1)}$ (see figure 4) with fixed orientation five windows corresponding to the number of vertices. The five windows can be constructed from $w(a)$ by rewriting this window as $w(q) = w(a,1) - (q - a)$ seen from its set of five Voronoi centres q given in equation (9).

We obtain

$$
\begin{aligned}
w(a,1)+a_1 &= (P(+0--0)) \cap (a_1 - a_2 + P(-+-00)) \cap (a_1 - a_5 + P(-00-+)) \\
&= (P(+0--0)) \cap (P(+--00)) \cap (P(+00--)) \\
w(a,1)+a_2 &= (a_2 - a_1 + P(+0--0)) \cap (P(-+-00)) \cap (a_2 - a_5 + P(-00-+)) \\
w(a,1)+a_3 &= (a_3 - a_1 + P(+0--0)) \cap (a_3 - a_2 + P(-+-00)) \\
&\quad \cap (a_3 - a_5 + P(-00-+)) \\
&= (P(-0+-0) \cap (P(--+00) \cap (a_3 - a_5 + P(-00-+)) \\
w(a,1)+a_4 &= (a_4 - a_1 + P(+0--0)) \cap (a_4 - a_2 + P(-+-00)) \\
&\quad \cap (a_4 - a_5 + P(-00-+)) \\
&= (P(-0-+0) \cap (a_4 - a_2 + P(-+-00)) \cap P(-00+-) \\
w(a,1)+a_5 &= (a_5 - a_1 + P(+0--0)) \cap (a_5 - a_2 + P(-+-00)) \cap (P(-00-+)).
\end{aligned}
\tag{10}
$$

In these expressions we have in a second step by application of equation (6) and its rotated versions eliminated all the translations which provide another boundary of the chosen Voronoi cell. In particular, the window $w(a,1)+a_1$ is an intersection of unshifted boundaries. This window was given in figure 4 (left) and corresponds to the filling of $D_{\parallel}^{(a,1)}$ in figure 4 (right) seen from the top vertex. In all other cases the window in the Voronoi domain is an intersection cone that involves one or two translated boundaries. We show the position of all five window cones from equation (10) in figure 5(*a*). There is a one-to-one correspondence between the hole position of the window cone and a vertex in the filling.

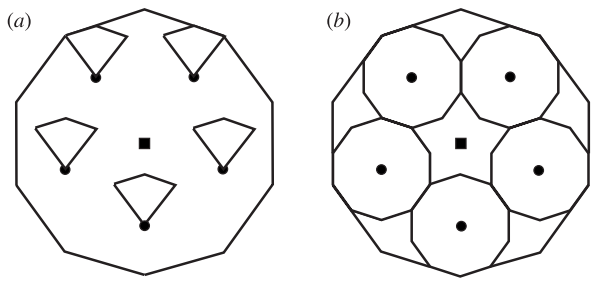

Figure 5. (*a*) Five cones $w(a,1)$ at hole positions $(h, r(h)) = (a,1)$ in $V_\perp$ are the windows for the filling $D_{\parallel}^{(a,1)}$ seen from its five vertices. (*b*) Fivefold rotations and superposition of the cones in (*a*) generate the total window for all holes of class $(a,1)$. The total window consists of five scaled decagons $\tau^{-2}V_\perp$ centred at the five hole positions of class $(h, r(h)) = (a,1)$.

3.2.3. Total window for all orientations and hole class (a, 1). Each cone in equation (10) is the window of a filled Delone cluster $D_{\parallel}^{(a,1)}$ of the same fixed orientation but seen from a different vertex. Any new orientation obtained by fivefold rotation yields in the Voronoi window another set of five window cones. The reflection (25)(34) transforms both the initial windows and the filling in figure 5 into itself. The total window under all these operations can be described as follows: it consists of five decagons centred at the five hole positions and scaled linearly in comparison to the Voronoi window as $\tau^{-2}V_\perp$. This total window is shown in figure 5(*b*).

3.2.4. Windows for the hole class $(a, 4)$. Finally, we apply the inversion i. The five hole positions $(h, r(h)) = (a, 1)$ go into five hole positions of the class $(h, r(h)) = (a, 4)$. There are five new decagonal windows and five new orientations of the filled Delone cluster $D^a_\parallel$. These windows and fillings are not shown in the figures.

We summarize the results on the Delone clusters D^a:

Proposition 2. *The Delone clusters* $D^{(a,j)}_\parallel$ *have a unique filling. The filling has a mirror symmetry and appears in 10 orientations, five for class* $(h, r(h)) = (a, 1)$ *and five for class* $(h, r(h)) = (a, 4)$. *The total windows for all orientations are scaled decagons* $\tau^{-2}V_\perp$, *centred at all hole positions* $h = a$ *of and intersected with* $V_\perp$.

3.3. Delone clusters $D^b_\parallel$ *and their windows*

We start again from the window side. The tiles X_1, X_2 each have three vertex holes of type b. Therefore, we find from the standard positions equation (6) a variety of vectors t. Again we denote by $X_l(b, j)$ the coding tiles in coordinates seen from the fixed hole position and by $X^*_l(b, j)$ the duals. In section 2 we mentioned that the point group elements $g \in I_2(5)$ applied with respect to hole positions are symmetries of the lattice. In table 2 we apply the inversion i, which does not belong to $I_2(5)$, with respect to hole positions. Instead of introducing a second set of standard 2-boundaries we have extended proposition 1. The interpretation is that i acts geometrically on the standard rhombus tiles and their duals but at the same time according to definition 1 interchanges the subclasses of holes $(a1, a4)$ and $(b3, b2)$ at the vertices of the rhombus tiles compared with their labels given in figure 9. In the intersection figure 6 this combined action ensures that all the intersecting rhombus tiles share the hole vertex of class $(b, 3)$.

3.3.1. The window for fixed orientation and hole class $(b, 3)$. Upon choosing a fixed orientation we find the expressions as in table 2.

Table 2.

Tiles $X_1(b, 3)$, $X^*_1(b, 3)$		
t	$(-a_3 - a_4)$	$(a_1 + a_2)$
g	(12345)	i(14253)
$gX(b, 3)$	$a_4 + a_5 + P(0+0--)$	$a_4 + a_5 + P(++0-0)$
$gX^*(b, 3)$	$a_4 + a_5 + \langle 0, a_2 - a_4, a_2 - a_5\rangle$	$a_4 + a_5 + \langle 0, -a_4 + a_2, -a_4 + a_1\rangle$
t	$(a_1 + a_5)$	$(a_1 + a_5)$
g	i(15432)	i(13524)
$gX(b, 3)$	$a_4 + a_5 + P(0++0-)$	$a_2 + a_3 + P(+0-0+)$
$gX^*(b, 3)$	$a_4 + a_5 + \langle 0, -a_5 + a_2, -a_5 + a_3\rangle$	$a_2 + a_3 + \langle 0, -a_3 + a_1, -a_3 + a_5\rangle$
Tiles $X_2(b, 3)$, $X^*_2(b, 3)$		
t	$(-a_2 - a_5)$	$(-a_2 - a_5)$
g	(13524)	e
$gX(b, 3)$	$a_2 + a_4 + P(0-+-0)$	$a_2 + a_5 + P(+-0\,0-)$
$gX^*(b, 3)$	$a_2 + a_4 + \langle 0, a_3 - a_4, a_3 - a_2\rangle$	$a_2 + a_5 + \langle 0, a_1 - a_2, a_1 - a_5\rangle$
t	$(a_1 + a_4)$	
g	i(14253)	
$gX(b, 3)$	$a_2 + a_4 + P(0\,0+-+)$	
$gX^*(b, 3)$	$a_2 + a_4 + \langle 0, -a_4 + a_5, -a_4 + a_3\rangle$	

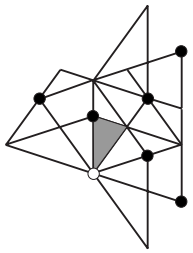

Figure 6. The window $w(b, 3)$ is the shaded intersection cone of seven rhombus tiles attached to a hole $(h, r(h)) = (b, 3)$, open circle. The seven tiles are marked in addition by their holes $h = a$, full circles. The filling $D_{\parallel}^{(b,3)}$ is shown in figure 7.

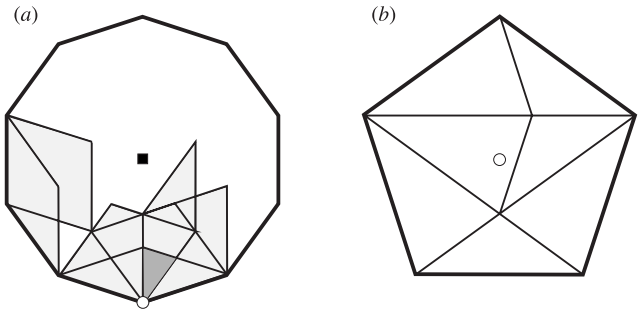

Figure 7. (*a*) Window cone $w(b, 3)$, shaded, equation (11), as the intersection of rotated and translated rhombus tiles $X_{1\perp}, X_{2\perp}$ at a hole position $(b, 3)$, open circle, in the decagon $V_{\perp}$. (*b*) Filled pentagonal Delone cluster $D_{\parallel}^{(b,3)}$ as the union of dual rotated and translated triangles $X_{1\parallel}^{*}, X_{2\parallel}^{*}$.

The window $w(b, 3)$ is obtained as the intersection of the seven rhombus tiles in table 2. It is a cone of opening angle $2\pi/10$ and part of a scaled decagon $\tau^{-2}V_{\perp}$ (cf figure 6).

Again we ask about the occurrence of the filling $D_{\parallel}^{(b,3)}$ in the tiling and look into the relation of its window in figure 6 with the Voronoi window. It is not possible to represent the window $w(b, 3)$ as the intersection of rhombus boundaries of a single Voronoi cell. Seen from the point of view of the tiling, the reason is that in $D_{\parallel}^{(b,3)}$ figure 7 there is no vertex q shared by all the tiles X_j^{*} of the filling, in contrast to $D_{\parallel}^{a}$. To represent the window $w(b, 3)$ within $V_{\perp}$ we must admit rotated and translated rhombus tiles in a single decagon. One such representation is given in equation (11) and shown in figure 7.

The window and filling for $q - b = -a_2 - a_5$ is given by

$$\begin{aligned}
w(b,3) - a_2 - a_5 &= (-a_2 + a_4 + P(++0-0)) \cap (-a_2 + a_4 + P(++0-0)) \\
&\quad \cap (-a_2 + a_4 + P(0++0-)) \cap (a_3 - a_5 + P(+0-0+)) \\
&\quad \cap (a_4 - a_5 + P(0-+-0)) \cap P(+-00-) \\
&\quad \cap (a_4 - a_5 + P(+-00-)) \\
D_{\parallel}^{(b,3)} &= (-a_2 + a_4 + \langle 0, a_2 - a_4, a_2 - a_5\rangle) \cup (-a_2 + a_4 + \langle 0, -a_4 + a_2, -a_4 + a_1\rangle) \\
&\quad \cup (-a_2 + a_4 + \langle 0, -a_5 + a_2, -a_5 + a_3\rangle) \cup (a_3 - a_5 + \langle 0, -a_3 + a_1, -a_3 + a_5\rangle) \\
&\quad \cup (a_4 - a_5 + \langle 0, a_3 - a_4, a_3 - a_2\rangle) \cup \langle 0, a_1 - a_2, a_1 - a_5\rangle \\
&\quad \cup (a_4 - a_5 + \langle 0, -a_4 + a_5, -a_4 + a_3\rangle).
\end{aligned} \tag{11}$$

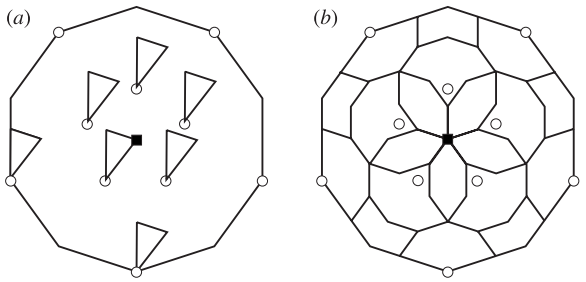

Figure 8. (*a*) Seven cones $w(b, 3)$ at hole positions $(b, 3)$ in $V_\perp$ are the windows for the filling $D_\parallel^{(b,3)}$ seen from its seven vertices. (*b*) Fivefold rotations, the reflection (25)(34) in the vertical line, and superposition of the cones in (*a*) generate the total window for all holes of class $(b, 3)$, open circles. The total window consists of ten scaled decagons $\tau^{-2}V_\perp$, centred at ten hole positions $(b, 3)$ and intersected with $V_\perp$.

3.3.2. All windows for fixed orientation of hole class $(b, 3)$. We evaluate, seen from the hole vertex, all the Voronoi centres which appear in table 2 as vertices of any $X_1^*(b)$, $X_2^*(b)$ to obtain

$$q - b = a_1 + a_2, a_1 + a_5, a_2 + a_3, a_2 + a_4, a_2 + a_5, a_3 + a_4. \tag{12}$$

The seven positions $b - q$ are holes of class $(h, r(h)) = (b, 3)$ but do not exhaust the representatives of this class within one Voronoi cell. By the same reasoning as before, the seven vectors $b - q$ produce seven window cones $w(b) + b - q$ on $V_\perp$. In the tiling they correspond to the seven vertices of the filling $D_\parallel^b$ (see figure 7). These windows are shown in figure 8(*a*). Again there is a one-to-one relation between the hole position of a window cone and a vertex of the filling. The filling has two internal vertices. They correspond to window cones at hole positions on vertices of the decagon.

3.3.3. Total window for all orientations of hole class $(b, 3)$. Applying all fivefold rotations to the seven windows one obtains altogether $7 \times 5 = 35$ window cones, located now at all 10 holes of type $(b, 3)$ of the Voronoi cell. Next, include the reflection (25)(34) which still keeps the same class of holes. Both the initial seven windows $w(b, 3)$ and the initial filling $D_\parallel^{(b,3)}$ go into different reflected forms. Under fivefold rotation the reflected window cones fit precisely in between the first 35 window cones and fill up the scaled decagons. The total window can now be described as follows: first, consider scaled decagons $\tau^{-2}V_\perp$ at all 10 representative hole positions. Drop from these decagons all the sectors which fall outside of $V_\perp$. The total number of cones is $5(10 + 4) = 70$. This total window is shown in figure 8. By comparison with the previous section we observe that the window cones $w(b, 3)$ at all hole positions on the edges of the decagon $V_\perp$ correspond to internal vertices of the Delone filling $D_\parallel^{(b,3)}$.

3.3.4. Windows for hole class $(b, 2)$. Next apply the inversion i. It transforms the 10 holes from class $(b, 3)$ to class $(b, 2)$ and, together with the reflection (25)(34), gives a new total window. To these windows there correspond 10 more rotated fillings $D_\parallel^{(b,2)}$. They are not shown in the figures.

We summarize the results on the Delone clusters D^b:

Proposition 3. *The Delone clusters $D_\parallel^b$ have a unique filling. It has no point symmetry with respect to its centre and appears in 20 orientations, 10 for class* $(b, 3)$ *and 10 for class* $(b, 2)$. *The windows for all orientations are scaled decagons $\tau^{-2}V_\perp$, centred at all hole positions $h = b$ of and intersected with $V_\perp$.*

4. Covering by Delone clusters

Given a vertex of the tiling $(\mathcal{T}^*, A_4)$, does it always belong to at least one Delone cluster? Are all the tiles of the tiling covered by Delone clusters, and what is the covering fraction? We analyse these points in this section.

4.1. Covering of vertices and tiles

We analyse the covering of a vertex $q_\parallel \subset (\mathcal{T}^*, A_4)$ from the side of the window. In terms of the windows this vertex is covered if and only if $q_\perp$ belongs to the window of at least one Delone cluster.

Proposition 4 (Window criterion for covering of vertices). *Any vertex $q_\parallel$ in the tiling $(\mathcal{T}^*, A_4)$ is covered by a Delone cluster $D^h_\parallel$ if and only if $q_\perp \in V_\perp$ is covered by a window $w(h)$.*

To check what fraction of vertices in the tiling is covered by some Delone cluster one must superpose the total windows for all four hole classes. Note that these windows include the occurrence of fillings seen from any one of their vertices. It is easy to see from figures 5, 8 and their versions rotated by $2\pi/10$ that the four total windows together cover all the points of the decagon $V_\perp$. As a result we find

Proposition 5 (Delone covering of all vertices). *Any vertex of the tiling $(\mathcal{T}^*, A_4)$ is covered by at least one Delone cluster.*

Consider next the Delone covering for complete tiles of the tiling. A tile $X^*_\parallel$ at the vertex $q_\parallel$ occurs in the tiling whenever $q_\perp \in X_\perp \subset V_\perp$. If moreover $q_\perp \subset w(h)$ then it follows that $X^*_\parallel \subset D^h_\parallel$.

Proposition 6 (Window criterion for covering of tiles). *A tile $X^*_\parallel$ in the tiling is completely covered by at least one Delone cluster if and only if its window $X_\perp \in V_\perp$ is completely covered by all the windows $w(h)$ for the local hole vertices $h_\perp \in X_\perp$.*

As can be seen in figure 9, the criterion proposition 6 is fulfilled from the window side for all the tiles of the triangle tiling. There follows

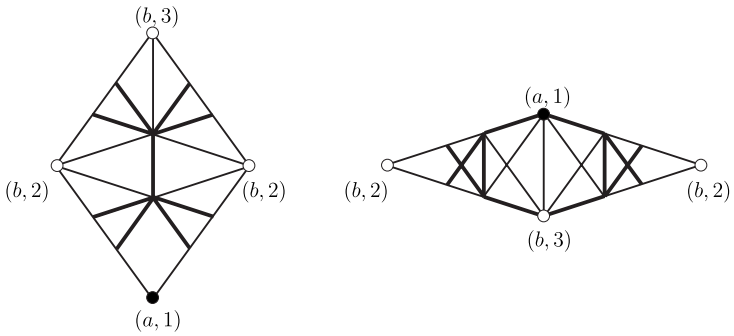

Figure 9. The two rhombus tile windows $X_{1\perp}$, $X_{2\perp}$ are completely covered by cones from small decagons (heavy edge lines) centred at the hole positions marked (a, j), (b, l) (full and open circles) on their four vertices.

Proposition 7 (Delone covering of all tiles). *Any tile of the tiling* $(\mathcal{T}^*, A_4)$ *is completely covered by at least one Delone cluster.*

A patch of the triangle tiling along with the Delone clusters is given in figure 5 of [8].

4.2. Covering fraction

All vertices and all tiles of the tiling were found to be covered by Delone clusters. To quantify the efficiency of this covering we use, in analogy with the packing fraction, the following definition.

Definition 4. *Consider a large patch of the tiling and its covering Delone clusters. The covering fraction* $f_{\rm cov}$ *we define as the limit for infinite patch size of the ratio between the area* $F_{\rm cov}$ *of all Delone clusters on the patch and the area* F *taken by the patch.*

A proper tiling would yield a covering fraction $f_{\rm cov} = 1$. For the covering by Delone clusters we expect a value larger than 1 due to overlap. Consider a large patch of area F of the tiling built from acute triangles $X^*_{1\|}$ and obtuse triangles $X^*_{2\|}$. Let $n(1), n(2)$ denote the number of these tiles for fixed orientation in the patch. The windows of the two tiles are the thick and the thin Penrose rhombus. The relative frequencies of the two tiles in the infinite-tiling limit are proportional to the area taken by their windows. We put arrows in front of asymptotic values valid for large but finite patches and have

$$n(1)/n(2) \to \tau. \tag{13}$$

The area F of the patch can be written in terms of the tiles as

$$\begin{aligned} F &:= 10(n(1)|X^*_{1\|}| + n(2)|X^*_{2\|}|) \\ &\to 10(\tau^2+1)n(2)|X^*_{2\|}|. \end{aligned} \tag{14}$$

The factor of 10 accounts for the possible orientations. In the second line we used equation (13) and $|X^*_{1\|}|/|X^*_{2\|}| = \tau$. Let $n(q)$ denote the number of vertices in the patch. To relate this number to the number of tiles we attach to each vertex of a tile the fraction, internal angle/(2π) at the vertex. Up to the boundaries of the patch these fractions add up to the number $n(q)$ of vertices, and so they must yield the correct asymptotics. Inside any triangle tile the internal angles sum to π and so contribute the fraction $\frac{1}{2}$ to the number of vertices. Therefore, we can write with equation (13)

$$n(q) \to \left(\tfrac{10}{2}\right)(n(1)+n(2)) \to \left(\tfrac{10}{2}\right)\tau^2 n(2). \tag{15}$$

With these results we obtain from equations (14) and (15)

$$F \to 2\tau^{-2}(\tau^2+1)n(q)|X^*_{2\|}| \tag{16}$$

valid for $n(q) \gg 1$.

We turn to the Delone clusters and wish to relate the area covered by them to the number $n(q)$ of vertices in the patch. The area of the Delone clusters is, respectively,

$$\begin{aligned} |D^a| &= |X^*_{1\|}| + 2|X^*_{2\|}| = (\tau+2)|X^*_{2\|}| \\ |D^b| &= 4|X^*_{1\|}| + 3|X^*_{2\|}| = (4\tau+3)|X^*_{2\|}|. \end{aligned} \tag{17}$$

Let $n(a,1), n(a,4), n(b,3), n(b,2)$ denote the number of oriented Delone clusters in the patch. These numbers take asymptotic values given by the ratio of the windows of the Delone clusters to $|V_\perp|$, multiplied by the number of vertices,

$$5n(a,1), 5n(a,4) \to \tau^{-4}n(q),\ 10n(b,3),\ 10n(b,2) \to \tau^{-4}n(q). \tag{18}$$

The numbers 5 and 10 count the possible orientations of the two Delone clusters. Then the area covered by all Delone clusters on the patch is from equations (17) and (18)

$$F_{\rm cov} := 5(n(a,1)+n(a2))|D^a| + 10(n(b,3)+n(b,2))|D^b|$$
$$\to 2\tau^{-4}n(q)(|D^a|+|D^b|) = 10\tau^{-2}n(q)|X^*_{2\|}| \tag{19}$$

again valid for $n(q) \gg 1$. From equations (19) and (16) we can now compute the covering fraction according to definition 4 as the limit

$$f_{\rm cov} = \lim_{n(q)\to\infty}(F_{\rm cov}/F) = (10\tau^{-2})/(2\tau^{-2}(\tau^2+1)) = 5/(\tau+2) = 1.38. \tag{20}$$

So on average there is an excess of 38% in the covering of the triangle tiling by Delone clusters.

5. Fundamental domain property

We inquire whether the Delone clusters can be related to a fundamental domain. In [8] the notion of a fundamental domain $\mathcal{F}(\mathcal{T}, \Lambda)$ was given for functions compatible with a class of quasiperiodic tilings, built from a minimal set of prototiles and their translates. The tiling

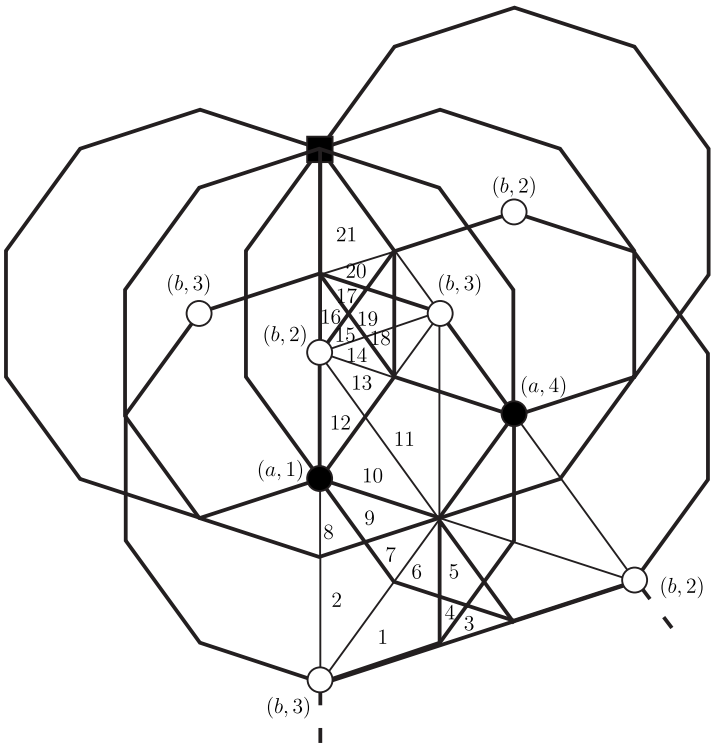

Figure 10. A sector of opening angle $2\pi/10$ of the decagon window $V_\perp$. Small decagons (heavy lines) around eight hole positions marked $(a,1)$, $(a,4)$, $(b,3)$, $(b,2)$ are the windows of eight Delone clusters, with sectors (thin lines) corresponding to possible orientations. The small decagons and their sectors intersect in 21 numbered polygons, up to a reflection $i(15)(24)$ in the symmetry axis of the large sector. Each polygon is the window for a set of Delone clusters linked by a shared vertex. The patches of linked Delone clusters can be constructed from the small decagon sectors which participate in the polygonal window. They are shown in figure 11.

$(\mathcal{T}, A_4)$ belongs to this class. As prototiles we may choose the two triangles $X^*_{1\|}$, $X^*_{1\|}$, each in 10 possible orientations. A possible fundamental domain $\mathcal{F}(\mathcal{T}, A_4)$ is then given by all points from these 20 prototiles.

As shown in figure 5 of [8], it is possible to choose filled oriented Delone clusters for four different hole classes which encompass all of these 20 prototiles.

Proposition 8. *Four filled Delone clusters of the four hole classes* $(a, 1)$, $(a, 4)$, $(b, 3)$, $(b, 2)$ *can be oriented so that they form a fundamental domain* $\mathcal{F}(\mathcal{T}^*, A_4)$ *for quasiperiodic functions compatible with the tiling* $(\mathcal{T}^*, A_4)$.

6. Linkage of Delone clusters

How are the Delone clusters linked in the covering of the tiling? Consider the linkage of Delone clusters by a shared vertex $q_\| \in \cup_h D^h_\|$ of the tiling. From the window side this linkage is characterized by the condition $q_\perp \in \cap_h w(h) \subset V_\perp$. By constructing all possible intersections of the windows $w(h) \subset V_\perp$ we can find all linkages of Delone clusters by a vertex. Any window $w(h)$ is a sector of a small decagon around the hole position $h_\perp$. Inside $V_\perp \subset E_\perp$ we must find all possible intersections of these small decagons. It suffices to analyse a large sector of opening angle $2\pi/10$ of $V_\perp$. Such a sector is shown in figure 10. The small decagon windows around eight hole positions in $V_\perp$ contribute to the large sector.

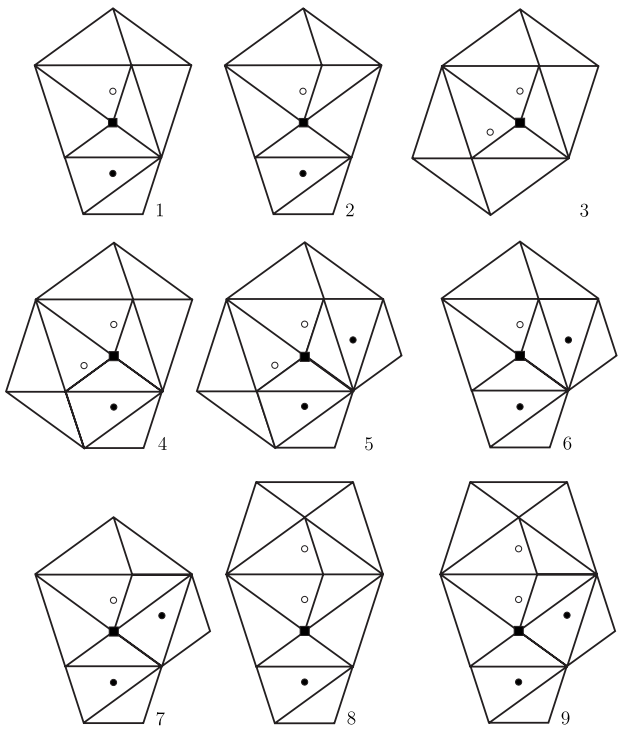

Figure 11. The Delone clusters form 21 linkages by a vertex shown in the figure. Their windows are the 21 numbered polygons of figure 10. The linking vertex is marked by a full square, the centres of the Delone clusters are marked for holes of type a, b by full and open circles. Seven linkages are invariant under the reflection $i(15)(24)$, 14 more linkages (not shown) result from the action of this reflection on the remaining ones.

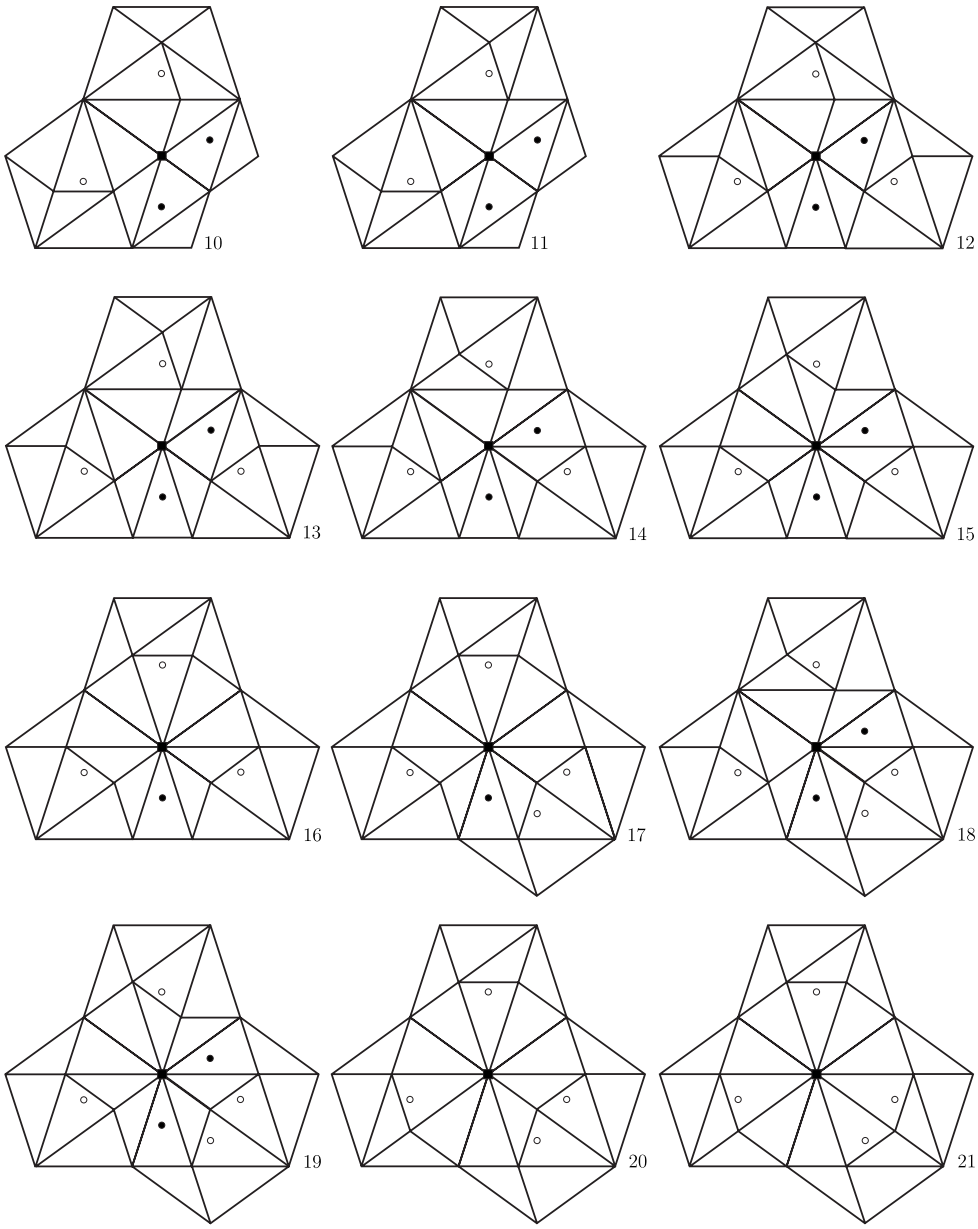

Figure 11. Continued.

There are 21 intersection polygons which form the windows for linked Delone clusters. The reflection $i(15)(24)$ in the symmetry axis of the sector interchanges subclasses of holes. The seven intersection polygons $3, 5, 11, 18 - 21$ are invariant under this reflection, the other 14 have images in the sector under this reflection. For each hole that contributes to an intersection polygon we determine its centre position and the specific sector of its decagon. The specific sector is obtained from a standard sector of figures 3 or 6 by a point group element g.

Table 3. Centres of Delone clusters in the linkages $j = 1, \ldots, 21$, and their orientations. Rows 2−9 list the centres and the orientations, expressed by the action of $s_1 =: (25)(34)$, $g_5 =: (12345)$, i on the standard positions in figures 4 and 7. Row 10 gives the relative frequency $\nu(j)$ and row 11 under vert the central vertex configuration in the enumeration of [1, p 2243].

	h	1	2	3	4	5	6	7	8	9	10	11
$(a, 1)$	a_1	g_5^4	g_5^4	—	g_5^4	g_5^4	g_5^4	g_5^4	g_5^4	g_5^4	g_5^2	g_5^2
$(a, 4)$	$-a_5$	—	—	—	—	i	i	$g_5^2 i$	—	$g_5^2 i$	$g_5^2 i$	$g_5^2 i$
$(b, 3)$	$-a_2 - a_5$	$g_5^2 s_1$	e	$g_5^2 s_1$	$g_5^2 s_1$	$g_5^2 s_1$	$g_5^2 s_1$	e	e	e	—	—
$(b, 3)$	$-a_2 - a_3$	—	—	—	—	—	—	—	—	—	$g_5 s_1$	$g_5 s_1$
$(b, 3)$	$-a_4 - a_5$	—	—	—	—	—	—	—	—	—	—	—
$(b, 2)$	$a_1 + a_4$	—	—	$g_5^2 i$	$g_5^2 i$	$g_5^2 i$	—	—	—	—	—	—
$(b, 2)$	$a_3 + a_4$	—	—	—	—	—	—	—	$s_1 i$	$s_1 i$	$s_1 i$	$g_5^3 i$
$(b, 2)$	$a_1 + a_2$	—	—	—	—	—	—	—	—	—	—	—
$\nu(j)$		$2\tau^{-7}$	$2\tau^{-7}$	τ^{-9}	τ^{-10}	$2\tau^{-9}$	τ^{-8}	τ^{-8}	τ^{-8}	τ^{-7}	τ^{-6}	$2\tau^{-7}$
vert		1	2	1	1	1	1	2	2	2	3	3

	h	12	13	14	15	16	17	18	19	20	21
$(a, 1)$	a_1	e	e	e	e	e	e	e	e	—	—
$(a, 4)$	$-a_5$	$g_5^2 i$	$g_5^2 i$	$g_5^4 i$	$g_5^4 i$	—	—	$g_5^4 i$	$g_5^4 i$	—	—
$(b, 3)$	$-a_2 - a_5$	—	—	—	—	—	—	—	—	—	—
$(b, 3)$	$-a_2 - a_3$	g_5	g_5	g_5	$g_5^3 s_1$	$g_5^3 s_1$	$g_5^3 s_1$	g_5	$g_5^3 s_1$	g_5^3	g_5^3
$(b, 3)$	$-a_4 - a_5$	$g_5^4 s_1$	$g_5^4 s_1$	g_5^2	g_5^2	g_5^2	g_5^2	g_5^2	g_5^2	g_5^2	$g_5^2 s_1$
$(b, 2)$	$a_1 + a_4$	—	—	—	—	—	—	—	—	—	—
$(b, 2)$	$a_3 + a_4$	$s_1 i$	$g_5^3 i$	$g_5^3 s_1 i$	$g_5 i$	$g_5 s_1 i$	$g_5 s_1 i$	$g_5^3 s_1 i$	$g_5 i$	$g_5 s_1 i$	$g_5 s_1 i$
$(b, 2)$	$a_1 + a_2$	—	—	—	—	—	$g_5^2 s_1 i$	$g_5^2 s_1 i$	$g_5^2 s_1 i$	$g_5^2 s_1 i$	$g_5^2 i$
$\nu(j)$		τ^{-7}	τ^{-8}	τ^{-9}	τ^{-10}	τ^{-9}	τ^{-10}	τ^{-10}	$\tau^{-11}(\tau + 2)$	τ^{-9}	τ^{-6}
vert		4	4	5	6	7	7	5	6	8	9

We pass to the tiling in $E_\parallel$, mark the centre position of the hole, and apply the group element g to the standard position in figures 4 or 7 of the filled Delone cluster. As a result we find the 21 sets of Delone clusters linked by a vertex and shown in figure 11. The central part of any linkage is a vertex configuration of the tiling $(\mathcal{T}^*, A_4)$ as classified in [1]. Observe that for any vertex configuration the covering enforces the continuation into a few linkages of Delone clusters. The reflection $i(15)(24)$, applied now in $E_\parallel$, leaves seven linked clusters invariant and produces 14 new images (not shown) with interchanged subclasses of holes. Finally, these linkages can appear in all orientations under $I_2(5)$. For each linkage one can compute the area of the window or intersection polygon and divide it by the area of the large sector. The resulting number $\nu(j)$ yields the relative frequency of occurrence for the linkage j in the tiling. All the relevant quantities are listed in table 3.

The information on the linkages is exhaustive. Other aspects, such as for example the linkage in pairs of Delone clusters, could easily be derived from it.

References

[1] Baake M, Kramer P, Schlottmann M and Zeidler D 1990 Planar patterns with fivefold symmetry as sections of periodic structures in 4-space *Int. J. Mod. Phys.* B **4** 2217–68

[2] Grünbaum F and Shepard G C 1987 *Tilings and Patterns* (New York: Freeman)

[3] Conway J H and Sloane N J A 1988 *Sphere Packings, Lattices and Groups* (New York: Springer)

[4] Gummelt P 1996 Penrose tilings as coverings of congruent decagons *Geometriae Dedicata* **62** 1–17

[5] Humphreys J E 1990 *Reflection Groups and Coxeter Groups* (Cambridge: Cambridge University Press)

[6] Kramer P and Schlottmann M 1989 Dualization of Voronoi domains and Klotz construction: a general method for the generation of proper space filling *J. Phys. A: Math. Gen.* **22** L1097–102
[7] Kramer P, Quandt A, Schlottmann M and Schneider T 1995 Atomic clusters and electrons in the Burkov model of AlCuCo *Phys. Rev.* B **51** 8815–29
[8] Kramer P 1999 Quasicrystals: atomic coverings and windows are dual projects *J. Phys. A: Math. Gen.* **32** 5781–93
[9] Kramer P 1998 The decagon covering project *Proc. Mathematical Aspects of Quasicrystals (Paris, September 1998)* ed J-P Gazeau and L L Verger-Gaugry
[10] Kramer P 2000 Delone clusters and coverings for icosahedral quasicrystals *J. Phys. A: Math. Gen.* submitted
[11] Sommerville D M Y 1958 *An Introduction to the Geometry of N Dimensions* (New York: Dover)
[12] Jeong H-C and Steinhardt P J 1997 Constructing Penrose-like tilings from a single prototile and the implications for quasicrystals *Phys. Rev.* B **55** 3520–32